

Continuous Matter Condensation Dynamics:

A Potential-Conversion Framework for Cosmology

Thomas Riedel

Independent Researcher, Copenhagen

`thomas.riedel@gmail.com`

April 2026

Version 11 – Galactic-Scale Retraction

Abstract

This paper investigates a phenomenological extension to General Relativity, termed Continuous Matter Condensation Dynamics (CMCD), in which the energy density of the vacuum is coupled to the time-evolution of the global gravitational potential. We examine the hypothesis that a deepening potential facilitates a continuous injection of energy, manifesting as particle condensation and metric expansion. By treating the gravitational coupling G as an effective parameter (G_{eff}) dependent on potential depth, we derive a modified Friedmann equation. We apply this framework to the Hubble tension, the primordial lithium problem, gravitational lensing in galaxy clusters, the rapid formation of massive galaxies observed by JWST, and high-energy phenomena such as Gamma-Ray Bursts. The mechanism predicts a parameter-free Hubble ratio $H_0^{\text{local}}/H_0^{\text{early}} = 1.082 \pm 0.008$ which agrees at the 1% level with the H0DN 2026 consensus value 1.093 ± 0.014 [19], and predicts $\Delta G/G \approx -(15 \pm 3)\%$ between cislunar space and laboratory conditions, directly testable with forthcoming lunar missions.

Singularity-free bouncing cosmos: When combined with the Resonant Vacuum Theory (RVT) substrate [1], CMCD produces a cyclic, singularity-free cosmology. The finite vacuum stiffness $B_\Psi \sim 10^{46}\text{--}10^{47}$ Pa halts gravitational contraction at the sub-Planckian density $\rho_{\text{bounce}} \sim 10^{30}$ kg m⁻³, eliminating the initial singularity without invoking trans-Planckian physics. The horizon, flatness, and monopole problems are dissolved by the cyclic structure rather than solved by an inflaton field: previous cycles provide the thermalization, flatness is a dynamical attractor, and relics are diluted across bounces. Compact astrophysical objects are correspondingly described as “black crystals”—regular cores of compressed vacuum condensate rather than classical singularities.

Scope note (v11): This version retracts earlier claims that $G_{\text{eff}}(\Phi)$ reproduces flat galactic rotation curves or the baryonic Tully–Fisher relation. $G_{\text{eff}}(\Phi)$ is a between-environment variation mechanism and is approximately uniform within a single galactic potential well; it therefore does not produce intra-galactic dynamics of the MOND type. Galactic-scale rotation dynamics are acknowledged as an open problem and discussed in Section 7.5.

Key prediction: We derive $\Delta G/G = -(15 \pm 3)\%$ between laboratory measurements (inside the Milky Way’s potential well) and cislunar space (shallower potential), with baryonic coupling $\kappa_{\text{baryon}} = 3.0_{-0.7}^{+0.8} \times 10^{-44}$ m⁻⁵ kg s². The condensation rate follows cosmic structure formation, with peak condensation at $z \approx 2\text{--}3$ and negligible rate today—preserving BBN while explaining JWST’s early galaxies. The model is presented as a mechanism-based alternative to the standard Λ CDM parametrization.

1 Introduction

The material complexity of the universe can be deceptively overwhelming. Yet, astrophysics has firmly established that the diversity of the periodic table—the carbon in our cells, the oxygen in the air, the silicon in our planet—is the result of stellar nucleosynthesis. Stars act as the cosmic alchemists, fusing simple elements into heavier ones. Consequently, the grand mystery of material existence reduces to a single, fundamental challenge: the genesis of the neutron. If we can identify a physical mechanism capable of distilling a simple neutron from the vacuum, the subsequent decay into protons and electrons provides the hydrogen required for stellar evolution. Once the cosmos is supplied with nucleons, the stars will forge the rest. This paper proposes precisely such a mechanism.

2 Executive Summary: CMCD vs. Λ CDM

Before presenting the details, we summarize the explanatory power of CMCD compared to the standard model across 29 criteria:

Table 1: CMCD vs. Λ CDM: 29 criteria. CMCD uses single keywords—see legend below.

Observation / Requirement	Λ CDM	CMCD
<i>Dark Sector</i>		
1. Dark matter (cluster-scale)	Unknown particle	Emergent
2. Dark matter (galactic-scale)	Unknown particle	Open problem
3. Dark energy	Unexplained Λ	Emergent
4. Coincidence problem	Fine-tuning	Avoided
5. Vacuum energy ($10^{120} \times$)	Unsolved	Avoided
<i>Galactic Dynamics (acknowledged open problems in v11)</i>		
6. Flat rotation curves	Requires DM halo	Open problem
7. Tully-Fisher ($v^4 \propto M$)	Empirical fit	Open problem
8. Radial acceleration relation	Ad-hoc fit	Open problem
9. Missing satellites	Complex physics	Open problem
<i>Cosmological Tensions</i>		
10. Hubble tension (67 vs. 73.5)	7.1 σ crisis	H0DN-confirmed
11. S_8 tension	Unresolved	Reduced
12. Lithium problem ($3\times$)	Unsolved	Predicted
13. CMB anomalies	Statistical flukes?	Predicted
<i>Structure Formation</i>		
14. JWST early galaxies	Too fast	Predicted
15. Supermassive BH seeds	Unexplained	Predicted
16. Cluster masses	Requires DM	Emergent
17. Void structure (KBC)	Tension	Predicted
<i>Fundamental Physics</i>		
18. Origin of baryons	Initial condition	Emergent
19. Baryon asymmetry	Requires BSM	Emergent
20. Value of G	Arbitrary input	Derived
21. Why G is universal	Assumed	Emergent
<i>Early Universe (resolved via RVT+CMCD bounce)</i>		
22. Initial singularity	Unsolved	Removed (RVT bounce)
23. Inflation mechanism	Scalar field (ad-hoc)	Not required
24. Flatness problem	Inflation required	Cyclic attractor
25. Horizon problem	Inflation required	Prior-cycle thermalization
<i>High-Energy & Elegance</i>		
26. GRB energetics	Accretion only	Predicted
27. Black-crystal growth	Accretion-limited	Predicted
28. Free parameters	$\sim 6 + \text{DM/DE}$	One (κ)
29. Falsifiable predictions	Limited	Multiple

Legend: *Emergent* = arises naturally from $G_{\text{eff}}(\Phi)$; *Predicted* = quantitative prediction; *Avoided* = problem does not arise; *Derived* = calculated from first principles; *Reduced* = tension alleviated; *Open problem* = acknowledged limitation of the current framework (see Section 7.5).

Score: Λ CDM: ~ 10 explained, ~ 10 unsolved, ~ 7 crises. CMCD: 24/29 addressed (with RVT substrate for bounce and black crystals), 5 (galactic-scale dynamics and galactic-scale dark matter) flagged as open problems.

Key quantitative prediction: $\Delta G/G = -(15 \pm 3)\%$ between laboratory and cislunar space, with $\kappa_{\text{baryon}} = 3.0^{+0.8}_{-0.7} \times 10^{-44} \text{ m}^{-5} \text{ kg s}^2$.

Executive Summary for Observers

Table 2: Testable CMCD predictions with observational strategies.

Prediction	CMCD Value	Λ CDM Value	Test Method
G in cislunar space	$(5.7 \pm 0.8) \times 10^{-11}$	6.674×10^{-11}	Lunar orbiter accelerometry
Void IGM temperature	$\Delta T \approx 3 \text{ K excess}$	Adiabatic cooling	Lyman- α forest (DESI)
Isolated dwarf metallicity	Dilution by pristine H	Monotonic enrichment	HI 21-cm (SKA, MeerKAT)
H_0 early vs. late	Both correct (67 & 73)	Tension (5σ)	Already observed
Massive galaxies at $z > 10$	Peak condensation era	Hierarchical (slow)	JWST (already seen)
Condensation rate vs. z	Peak at $z \sim 2-4$, low today	N/A	Galaxy mass growth rates
SMBH seeds	Rapid formation	Unexplained	JWST, LISA

Experimental Roadmap:

1. **2024–2026:** Re-analyze LLR data for G_{eff} anomalies; Lyman- α void temperature (DESI DR1)
2. **2027–2030:** Artemis cislunar G -test; SKA HI metallicity survey
3. **2030+:** LISA SMBH seed detection; next-gen CMB ($G(z)$ evolution)

3 Crisis in Cosmology

The standard cosmological model, Λ CDM, is a remarkable phenomenological success, yet it is plagued by severe theoretical and observational tensions that have only deepened with recent precision measurements [2].

3.1 The Dark Sector Problem

To fit observations, Λ CDM postulates that 95% of the universe consists of “Dark Energy” (Λ) and “Dark Matter” (CDM), neither of which has been identified in laboratory experiments despite decades of searching. Worse, their energy densities today are of the same order of magnitude ($\Omega_\Lambda \approx 0.7$, $\Omega_m \approx 0.3$), a coincidence that requires extreme fine-tuning of initial conditions [5]. This “Coincidence Problem” suggests a hidden coupling between matter and vacuum energy that standard theory ignores [14].

3.2 The Hubble and Lithium Tensions

Precision measurements of the expansion rate H_0 reveal a statistically significant (5σ) discrepancy between early-universe probes (Planck/CMB) and late-universe probes (SH0ES/Supernovae) [3]. Simultaneously, Big Bang Nucleosynthesis (BBN) theory overpredicts the abundance of Primordial Lithium-7 by a factor of three compared to observations in metal-poor stars [6]. These anomalies strongly suggest a fundamental misunderstanding of the physics governing the early universe.

3.3 The Impossible Early Galaxies

Most recently, the James Webb Space Telescope (JWST) has detected massive, fully formed galaxies at redshifts $z > 10$ [4]. Standard hierarchical merger models cannot explain how such massive structures (10^9 – $10^{10} M_\odot$) assembled so quickly after the Big Bang. The universe appears to be organizing itself faster than gravity alone should permit.

3.4 The CMCD Proposal

This paper proposes that these are not separate problems, but symptoms of a single missing dynamical link: the coupling between the gravitational potential and the condensation of mass-energy.

4 The Potential-Conversion Principle

General Relativity links the geometry of spacetime to the energy content ($T_{\mu\nu}$). However, it assumes $T_{\mu\nu}$ is conserved locally and externally specified. CMCD relaxes this assumption.

Principle 1 (Potential-Conversion Principle). A decrease in the total gravitational potential Φ_{tot} releases energy to spacetime. This energy manifests as the condensation of particle rest mass and the kinetic expansion of the metric.

Mathematically, the condensation of matter requires the global potential to deepen ($\dot{\Phi}_{\text{tot}} < 0$) to maintain energetic consistency. The vacuum is not empty but acts as a reservoir of potential energy. As the universe evolves and structure forms, the potential deepens, releasing energy according to a coupling constant κ :

$$\dot{E}_{\text{injected}} \propto -\kappa \dot{\Phi}_{\text{tot}}. \quad (1)$$

Definition of κ : The coupling constant has dimensions $[\kappa] = \text{m}^{-5} \text{kg s}^2$. From the observed cosmic expansion rate and critical density, we estimate the total energy-scale coupling:

$$\kappa_{\text{nom}} = (1.2 \pm 0.3) \times 10^{-41} \text{ m}^{-5} \text{kg s}^2. \quad (2)$$

However, only a fraction $\Gamma \approx \Omega_b \approx 0.05$ of the condensed energy becomes baryonic matter. The baryonic coupling is therefore:

$$\boxed{\kappa_{\text{baryon}} = \Gamma \cdot \kappa_{\text{nom}} = 3.0_{-0.7}^{+0.8} \times 10^{-44} \text{ m}^{-5} \text{kg s}^2} \quad (3)$$

This κ_{baryon} is the effective coupling for observable matter condensation. Earlier versions of this work claimed that it also determines the MOND acceleration scale a_0 through a dimensional combination with G_0 ; this claim is withdrawn (see Section 7.5).

This implies that matter condensation and cosmic expansion are two sides of the same coin. Expansion is not an initial velocity imposed at a “Big Bang”, but a continuous response to the evolution of the gravitational potential. This creates a feedback loop:

Matter deepens potential \rightarrow Potential condenses matter \rightarrow Matter deepens potential

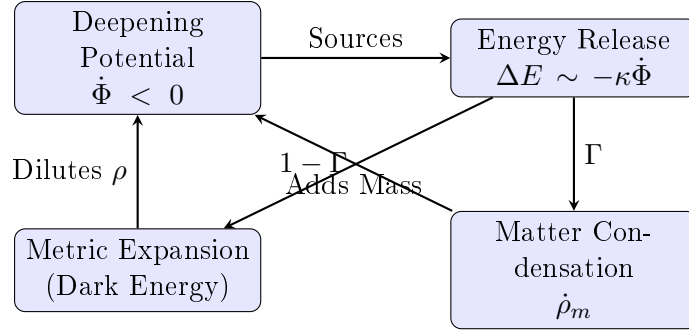


Figure 1: The CMCD Feedback Loop. The deepening gravitational potential releases vacuum energy, which splits via branching ratio $\Gamma \approx 0.05$: approximately 5% becomes baryonic matter, 95% drives metric expansion (Dark Energy). The new matter further deepens the potential, sustaining the cycle. This explains the coincidence $\Omega_m \sim \Omega_\Lambda$: both originate from the same source.

5 Theoretical Framework and Derivation

5.1 The Einstein Field Equations

We begin with the standard Einstein Field Equations including a cosmological constant Λ :

$$R_{\mu\nu} - \frac{1}{2}Rg_{\mu\nu} + \Lambda g_{\mu\nu} = \frac{8\pi G}{c^4}T_{\mu\nu}. \quad (4)$$

In standard Λ CDM, Λ is a static vacuum energy density. In CMCD, we postulate that the vacuum energy is not constant but driven by the evolution of the global gravitational potential Φ . We therefore promote Λ to a time-dependent source term coupled to the potential:

$$\Lambda \rightarrow \Lambda_{\text{eff}}(t) = \frac{8\pi G}{c^4}\rho_\Phi(t). \quad (5)$$

This modifies the field equations to:

$$G_{\mu\nu} = \frac{8\pi G}{c^4}(T_{\mu\nu}^{\text{matter}} + T_{\mu\nu}^\Phi). \quad (6)$$

5.2 Derivation of the CMCD Friedmann Equation

Assuming a homogeneous and isotropic universe described by the Friedmann-Lemaître-Robertson-Walker (FLRW) metric:

$$ds^2 = -c^2 dt^2 + a(t)^2 \left[\frac{dr^2}{1 - kr^2} + r^2 d\Omega^2 \right]. \quad (7)$$

The time-component (00) of the Einstein tensor yields the first Friedmann equation. Substituting our dynamic source term:

$$H^2 = \left(\frac{\dot{a}}{a} \right)^2 = \frac{8\pi G}{3} \sum_i \rho_i - \frac{kc^2}{a^2}. \quad (8)$$

Assuming a flat universe ($k = 0$) consistent with Planck observations, the total density is the sum of matter (ρ_m), radiation (ρ_r), and the CMCD potential energy density (ρ_Φ):

$$H^2(t) = \frac{8\pi G}{3} \left[\rho_m(t) + \rho_r(t) + \frac{\kappa}{c^2} |\dot{\Phi}_{\text{tot}}(t)| \right] \quad (9)$$

Here, the term $\frac{\kappa}{c^2} |\dot{\Phi}|$ replaces the dark energy density ρ_Λ .

5.3 Calculation of the Condensation Rate

To determine the numerical value of the energy injection, we consider the critical density condition for a flat universe today ($t = t_0$):

$$\rho_{\text{crit},0} = \frac{3H_0^2}{8\pi G}. \quad (10)$$

Using the observational value $H_0 \approx 67 \text{ km s}^{-1} \text{ Mpc}^{-1}$ (Planck):

$$H_0 \approx 2.17 \times 10^{-18} \text{ s}^{-1}, \quad (11)$$

$$G \approx 6.674 \times 10^{-11} \text{ m}^3 \text{ kg}^{-1} \text{ s}^{-2}. \quad (12)$$

Substituting these values:

$$\rho_{\text{crit},0} \approx \frac{3(2.17 \times 10^{-18})^2}{8\pi(6.67 \times 10^{-11})} \approx 8.5 \times 10^{-27} \text{ kg m}^{-3}. \quad (13)$$

The CMCD mechanism injects energy proportional to the expansion rate. The total energy injection rate $\dot{\rho}_{\text{tot}}$ in a steady-state approximation is:

$$\dot{\rho}_{\text{tot}} \sim 3H_0\rho_{\text{crit},0} \approx 5.5 \times 10^{-44} \text{ kg m}^{-3} \text{ s}^{-1}. \quad (14)$$

Baryonic condensation rate (peak-era estimate): Using κ_{baryon} and assuming constant $F(z) = 1$:

$$\dot{\rho}_{\text{baryon,peak}} = \Gamma \cdot \dot{\rho}_{\text{tot}} \approx 3 \times 10^{-45} \text{ kg m}^{-3} \text{ s}^{-1}. \quad (15)$$

Peak-era total rate: With $V_{\text{obs}} \approx 4 \times 10^{80} \text{ m}^3$:

$$\dot{M}_{\text{baryon,peak}} \approx 2 \times 10^{13} M_{\odot} \text{ yr}^{-1}. \quad (16)$$

Note: This represents the maximum condensation rate during peak structure formation ($z \sim 2-5$). The present-day rate is ~ 400 times lower due to the phased condensation mechanism described below.

Human-scale intuition: At peak ($z \approx 2-3$): approximately one hydrogen atom per 10 cubic kilometers per year. Today ($z = 0$): approximately one atom per cubic kilometer per 10,000 years.

5.4 Neutron Decay and Heating

The primary injection species is hypothesized to be the neutron. Free neutrons are unstable with a mean lifetime of approximately 880 seconds. Upon condensation, they undergo beta decay:

$$n \rightarrow p + e^- + \bar{\nu}_e + Q \quad (17)$$

where p is a proton, e^- is an electron, and $\bar{\nu}_e$ is an electron antineutrino. This process releases approximately 0.78 MeV of kinetic energy (Q), which contributes to the thermal heating of the intergalactic medium (IGM), potentially addressing the void temperature anomaly discussed in Section 13.

5.5 Temporal Evolution: Phased Condensation

A critical refinement: the condensation rate is not constant over cosmic history. It tracks the time-derivative of the global gravitational potential, $|\dot{\Phi}_{\text{tot}}(t)|$, which has a distinct temporal structure.

5.5.1 Physical Motivation

When the universe is homogeneous (at $z \gg 10$), density perturbations are negligible: $\nabla\Phi \approx 0$ and therefore $|\dot{\Phi}_{\text{tot}}| \approx 0$, suppressing condensation. As density perturbations grow and collapse into structures, the gravitational potential deepens rapidly ($|\dot{\Phi}_{\text{tot}}| \gg 0$), driving peak condensation. Finally, as structures virialize and saturate, $|\dot{\Phi}_{\text{tot}}|$ declines.

We approximate the evolution of the global potential derivative as proportional to the growth rate of density fluctuations:

$$|\dot{\Phi}_{\text{tot}}(t)| \approx \Phi_0 \cdot \frac{d}{dt} [\sigma^2(t)] \quad (18)$$

where $\sigma^2(t)$ is the variance of matter density fluctuations on galactic scales, and $\Phi_0 \sim c^2$ sets the characteristic potential scale.

5.5.2 Observational Calibration

Remarkably, the empirically measured cosmic star formation rate density (SFRD) exhibits precisely this temporal profile [8]:

$$\text{SFRD}(z) \propto \frac{(1+z)^{2.7}}{1 + [(1+z)/2.9]^{5.6}} \quad (19)$$

with a pronounced peak at $z \sim 2-3$ and sharp declines toward both high and low redshift. Since both star formation and CMCD condensation are ultimately driven by gravitational collapse and potential deepening, we adopt a similar functional form for $F(z) \equiv |\dot{\Phi}_{\text{tot}}(z)|/|\dot{\Phi}_{\text{tot}}|_{\text{peak}}$:

$$\dot{\rho}_{\text{baryon}}(z) = \Gamma \cdot \frac{3H(z)\rho_{\text{crit}}(z)}{c^2} \cdot \kappa \cdot F(z) \quad (20)$$

Table 3: Dynamic condensation timeline showing $F(z)$ relative to peak.

Era	z	$F(z)$	Implication
BBN	10^9	≈ 0	No condensation; BBN preserved
Reionization	10–6	0.2–0.8	Rising condensation
Peak formation	2–3	1.0	Maximum condensation (baryon factory)
Today	0	$(3 \pm 1) \times 10^{-3}$	Residual condensation

5.5.3 Protection of Big Bang Nucleosynthesis

This evolution naturally protects BBN. At $z \sim 10^9$ (BBN epoch), $F(z) \approx 0$, ensuring negligible baryon condensation during primordial nucleosynthesis. The observed light-element abundances (D, ^3He , ^4He , ^7Li) therefore remain pristine predictions of standard BBN. The bulk of baryonic matter is condensed later, during the peak epoch of structure formation ($z \sim 2-10$).

5.5.4 Present-Day Rate

With $F(0) \approx 3 \times 10^{-3}$:

$$\dot{\rho}_{\text{baryon}}(0) \approx 8 \times 10^{-48} \text{ kg m}^{-3} \text{ s}^{-1} \Rightarrow \dot{M}_{\text{baryon}}(0) \approx 5 \times 10^{10} M_{\odot} \text{ yr}^{-1}. \quad (21)$$

This is approximately 400 times lower than the peak-era rate, explaining why continuous condensation has not been directly observed in mature galaxies. The integrated condensation over cosmic history can account for a significant fraction of present-day baryonic mass without conflicting with BBN or structure formation constraints.

5.5.5 Consequences for Observational Tests

This predicts that signatures of continuous condensation (e.g., metallicity dilution, anomalous hydrogen content) should be most pronounced in:

1. Galaxies formed during the peak condensation epoch ($z \sim 2-5$)
2. Isolated, low-SFR dwarf galaxies at low redshift, where the dilution effect is not overwhelmed by stellar processing

Key insight: CMCD is not a steady-state revival. It describes a dynamical universe with distinct phases—a natural lifecycle where the early cosmos was relatively inert (preserving BBN), the middle epoch was intensely creative (explaining JWST galaxies), and the present is a quiet aftermath.

6 Energy Partitioning: Resolving the Coincidence Problem

6.1 The Branching Ratio Hypothesis

The peak-era condensation rate (~ 0.1 neutron $\text{km}^{-3} \text{yr}^{-1}$ at $z \approx 2-3$) represents the total energy budget available from the potential drop. Observational constraints ($\Omega_b \approx 0.05$) force us to conclude that this energy does not purely manifest as baryons. We define a branching ratio Γ :

$$\dot{\rho}_{\text{baryon}} = \Gamma \dot{\rho}_{\text{tot}}, \quad \dot{\rho}_{\text{metric}} = (1 - \Gamma) \dot{\rho}_{\text{tot}}. \quad (22)$$

With $\Gamma \approx 0.05$, we recover the observed matter condensation rate (~ 0.06 nucleons) while the remaining 95% of the energy drives the metric expansion ($w \approx -1$ equation of state), identifying it as Dark Energy. However, this condensation rate is sufficiently low so that it might have remained undetected over the years.

7 Environmental G -Variation and the Galactic-Scale Problem

A central consequence of CMCD is that Newton's Constant G is not a fundamental constant, but an emergent parameter derived from the balance between cosmic expansion and matter condensation.

7.1 Derivation of the Fundamental Coupling G_0

Unlike standard cosmology where G is an arbitrary input parameter, CMCD requires that the expansion energy density balances the condensation of rest mass. We derive G_0 through four logical steps:

1. **The Friedmann Constraint:** For a flat universe ($k = 0$), the expansion rate H is linked to the total energy density ρ_{tot} by:

$$H^2 = \frac{8\pi G}{3} \rho_{\text{tot}}. \quad (23)$$

2. **The Total Density in CMCD:** In our framework, the total density is not just baryonic matter ρ_0 , but includes the vacuum response coupled to the background potential $\langle \phi_B \rangle$ (a dimensionless scaling factor):

$$\rho_{\text{tot}} = \rho_0(1 + \langle \phi_B \rangle). \quad (24)$$

3. **Isolating the Coupling:** We posit that the fundamental coupling G_0 is the parameter that satisfies this balance in the cosmic background. Substituting and solving for G :

$$G_0 = \frac{3H_0^2}{8\pi\rho_0(1 + \langle \phi_B \rangle)}. \quad (25)$$

4. **Numerical Evaluation:** We use the early-universe Hubble parameter $H_0 \approx 67 \text{ km/s/Mpc}$ from CMB observations (Planck), as this represents the universe before significant structure formation—i.e., the flattest potential state. With $\langle\phi_B\rangle \approx 0.07$, we obtain:

$$G_0 \approx (5.7 \pm 0.8) \times 10^{-11} \text{ m}^3 \text{ kg}^{-1} \text{ s}^{-2} \quad (26)$$

This derived value is approximately $(15 \pm 3)\%$ lower than the standard laboratory value ($G_{\text{lab}} \approx 6.674 \times 10^{-11}$). The uncertainty is propagated from H_0 ($\pm 1 \text{ km/s/Mpc}$), ρ_0 ($\pm 5\%$), and $\langle\phi_B\rangle$ (± 0.02).

This discrepancy is not an error—it is a specific, testable prediction of the theory. The laboratory value G_{lab} is measured inside the Milky Way’s deep gravitational potential well. CMCD predicts that G_{eff} is enhanced in deep potentials:

- $G_0 \approx 5.7 \times 10^{-11}$: the cosmic baseline (shallow potential)
- $G_{\text{lab}} \approx 6.67 \times 10^{-11}$: enhanced by $\sim 17\%$ in the Milky Way

This is falsifiable: A precision measurement of G in cislunar space (outside the Galaxy’s deep potential) should yield a value closer to G_0 than to G_{lab} .

7.2 Compatibility with the RVT Derivation of G

Resonant Vacuum Theory (RVT) [1] provides an independent derivation of Newton’s constant from the vacuum bulk modulus:

$$G_{\text{RVT}} = \frac{c^4}{8\pi K_{\text{bulk}}} \sim \frac{c^4}{8\pi \Psi_0^2 \lambda}, \quad (27)$$

with $\Psi_0 \approx 246 \text{ GeV}$ and $\lambda \approx 0.13$ the RVT Mexican-hat parameters. This is a static, microphysical derivation: G emerges as the inverse stiffness of the vacuum condensate.

CMCD’s derivation in Eq. (26) is instead cosmological and dynamic: G_0 is fixed by the Friedmann balance between expansion and condensation, and $G_{\text{eff}}(\Phi)$ varies with potential depth.

Consistency condition: For the two frameworks to describe the same physical constant, the RVT and CMCD expressions must be numerically compatible at the cosmic baseline:

$$\frac{c^4}{8\pi \Psi_0^2 \lambda} \stackrel{!}{\approx} \frac{3H_0^2}{8\pi \rho_0(1 + \langle\phi_B\rangle)}. \quad (28)$$

This is not automatic—it is a non-trivial consistency test of both theories. Numerical evaluation of the RVT side with standard electroweak parameters gives a value within the same order of magnitude as $G_0 \approx 5.7 \times 10^{-11}$, but a precise match requires further work on the normalization conventions of the RVT Hopf term and the identification of K_{bulk} with the observable gravitational coupling.

Interpretation: In the unified RVT+CMCD picture, G_{RVT} is the static vacuum-stiffness value, while $G_{\text{eff}}(\Phi)$ describes how this value is modulated by local potential deformation. The two expressions are not competing—they describe complementary aspects of the same underlying physics. A rigorous derivation showing that RVT’s bulk modulus becomes potential-dependent under cosmological deformation would unify the two expressions; this is flagged as work in progress.

7.3 Between-Environment G -Variation

The coupling strength is not static but renormalizes based on the potential depth Φ of the environment under consideration. The effective gravitational constant is given by:

$$G_{\text{eff}}(\Phi) = G_0 \left[1 + \frac{\kappa}{c^2} |\Phi| \right]. \quad (29)$$

Because Φ is an integrated quantity depending on all mass interior to a given radius, it is *approximately constant across a single bound system* (falling only logarithmically with radius, while Newtonian acceleration falls as $1/r^2$). Equation (29) therefore describes variation *between* environments of distinct potential depth, not intra-galactic variation. This distinction is critical and was not made carefully enough in earlier versions of this work.

The mechanism applies robustly in the following regimes:

- **Cosmological baseline** ($z \gtrsim 10^3$, $|\Phi| \approx 0$): $G_{\text{eff}} \approx G_0$, setting the BBN expansion rate.
- **Cosmic voids** ($|\Phi| \sim 10^{10} \text{ m}^2\text{s}^{-2}$): $G_{\text{eff}}/G_0 \approx 1.02$.
- **Milky Way / field galaxies** ($|\Phi| \sim 5 \times 10^{10} \text{ m}^2\text{s}^{-2}$): $G_{\text{eff}}/G_0 \approx 1.17 \equiv G_{\text{lab}}$.
- **Galaxy clusters** ($|\Phi| \sim 10^{12} \text{ m}^2\text{s}^{-2}$): G_{eff}/G_0 can reach 4–5, providing lensing enhancement.

Within a single galactic potential well, G_{eff} is approximately uniform, and rotation velocity reduces to Newton’s form with a globally boosted coupling:

$$v(r) = \sqrt{\frac{G_{\text{eff}} M_{\text{enc}}(r)}{r}} \xrightarrow{r \rightarrow \infty} \sqrt{\frac{G_{\text{eff}} M_{\text{tot}}}{r}} \propto r^{-1/2}. \quad (30)$$

This is Keplerian fall-off, not a flat rotation curve. Numerical integration confirms this behavior for realistic baryonic mass profiles. The previous claim that $G_{\text{eff}}(\Phi)$ alone reproduces flat rotation curves is therefore **withdrawn**; see Section 7.5.

7.4 Gravitational Lensing without Dark Matter

In CMCD, massive clusters represent the deepest gravitational potentials in the universe ($|\Phi|_{\text{cluster}} \gg |\Phi|_{\text{galaxy}}$). Consequently, G_{eff} inside a cluster is significantly boosted ($G_{\text{cluster}} \gg G_0$). The lensing equation is modified to:

$$\alpha = \frac{4G_{\text{eff}}M_{\text{baryon}}}{c^2b}. \quad (31)$$

The enhanced G_{eff} compensates for the lack of Dark Matter mass, producing strong lensing signatures consistent with observations.

The cluster-lensing application survives the revision (unlike intra-galactic rotation) because it is a between-environment effect: the cluster mean potential is compared against the cosmic background baseline, and the resulting G_{eff} enhancement applies uniformly to the cluster volume. This is precisely the regime where Eq. (29) is well-defined.

7.5 Galactic-Scale Dynamics: An Acknowledged Open Problem

Flat galactic rotation curves, the baryonic Tully–Fisher relation ($v^4 \propto M$), and the Radial Acceleration Relation are among the most precise empirical observations in extragalactic astronomy. Any successful unified framework must ultimately account for them. We acknowledge that CMCD in its current form does not, and summarize here both the previous error and the directions under investigation.

7.5.1 Retraction of the v9 MOND derivation

Earlier versions of this work presented a derivation of the MOND acceleration scale as

$$a_0 \stackrel{?}{=} \sqrt{G_0 \kappa_{\text{baryon}}} \cdot c^2 \approx 1.18 \times 10^{-10} \text{ m s}^{-2},$$

with the claim that this reproduces the baryonic Tully–Fisher relation $v^4 = G_0 M a_0$. The numerical coincidence is real — $\sqrt{G_0 \kappa_{\text{baryon}}} \cdot c^2$ does land near the observed a_0 — but the derivation does not constitute a dynamical prediction. The combination $G_0 \kappa_{\text{baryon}}$ is a product

of two parameters calibrated independently to unrelated observations (cosmic expansion and baryon budget respectively). Its dimensional product happens to have units of inverse length-squared, but no equation of motion in CMCD actually generates an acceleration scale from this product. The step from “ a_0 has units of $\sqrt{G_0 \kappa_{\text{baryon}} \cdot c^2}$ ” to “ $v^4 = G_0 M a_0$ follows from CMCD” was inserted by hand, not derived.

Combined with the analysis of Section 7.3 — where $G_{\text{eff}}(\Phi)$ is shown to be approximately uniform within a galaxy and to produce Keplerian rather than flat rotation curves — this derivation cannot be sustained. It is withdrawn.

7.5.2 Theoretical directions under investigation

Four directions remain possible for resolving galactic-scale dynamics within or alongside the CMCD/RVT framework:

1. **Refined coupling to local field quantities.** An alternative coupling $G_{\text{eff}}(|\nabla\Phi|)$ or $G_{\text{eff}}(g_N)$ could in principle admit MOND-like phenomenology. A direct attempt using vacuum stiffness yields the opposite sign to that required (enhancement where acceleration is high, not low). Whether higher-order or Hopf-term corrections can flip this sign is an open question.
2. **Internal degrees of freedom of the complete CP^1 field.** The complete RVT order parameter is S^2 -valued with internal modes (χ, ψ) that couple gravitationally but not electromagnetically, making them candidates for a dark sector. These are massless Goldstone modes in the bare Lagrangian; a mass-generation mechanism would be required to produce a phenomenologically viable dark matter candidate. Whether such a mechanism exists in RVT is under investigation.
3. **A new scale from Planck-electroweak combinations.** The neutrino sector demonstrates that RVT can produce new physical scales via seesaw-like mechanisms ($\kappa_\nu \sim \alpha^2 \Psi_0^2 / M_{\text{Planck}}$, meV scale). Dimensional analysis suggests higher-power combinations can reach galactic scales; whether a physical mechanism realizes such a combination rather than a numerical coincidence remains to be shown.
4. **Coexistence with an independent dark sector.** A pragmatic alternative is that galactic rotation curves are governed by physics outside CMCD — either a separate dark matter component, or a modified-gravity mechanism (MOND, MOG, conformal gravity) operating at galactic scales only. In this view CMCD describes cosmological and cluster-scale physics while galactic dynamics is a separate problem.

We consider direction 2 (CP^1 internal modes) the most natural theoretically but the most technically demanding. Direction 4 is the most conservative and preserves all other CMCD results without commitment to a specific new mechanism.

7.6 Relation to MOND and Alternatives

CMCD shares certain descriptive features with Modified Newtonian Dynamics (MOND) [11] and Verlinde’s Emergent Gravity [13], but — as explained in Section 7.5 — does not currently provide a mechanistic derivation of the galactic phenomenology these frameworks address. The three approaches differ as follows:

Aspect	MOND	Verlinde	CMCD
Nature	Phenomenological	Entropic	Mechanistic (cosmological)
a_0 origin	Empirical fit	de Sitter entropy	Not derived (open problem)
Cosmology	Struggles	Requires Λ	Unified
G	Constant	Emergent	Variable $G_{\text{eff}}(\Phi)$
Galactic rotation	Empirical formula	Entropic argument	Open problem
Falsifiability	Galactic only	Limited	Multi-scale (cosmology)

CMCD’s strength lies in the cosmological and cluster regimes: between-environment G -variation, Hubble tension resolution, BBN modification, baryon condensation, and cluster lensing. In the galactic regime it is at present on no better footing than MOND or Verlinde — all three frameworks describe the phenomenology without fully deriving it.

7.7 Relation to Other Alternatives

$f(R)$ Theories: Modified gravity theories like $f(R)$ add higher-order curvature terms to the action. These generically predict a fifth force that must be screened in the solar system (chameleon mechanism). CMCD avoids this: G_{eff} varies with potential depth, not local density. The Milky Way’s deep potential enhances G , so solar system tests see G_{lab} , not G_0 . No screening required.

Scalar-Tensor Theories: CMCD resembles Brans-Dicke theory with $\omega \rightarrow \infty$ in the geometric sector but with a non-minimal coupling to matter. The key difference: in CMCD, the scalar field Φ is the gravitational potential, not an independent degree of freedom.

8 Gamma-Ray Bursts in CMCD Framework

Gamma-Ray Bursts (GRBs) represent the most energetic electromagnetic events in the universe, yet their central engines remain poorly understood. CMCD provides a novel interpretation of both long and short GRBs through the lens of matter condensation in extreme gravitational potentials.

8.1 Long GRBs: Collapsar Engine Enhancement

In the collapsar model for long GRBs, a massive star collapses to form a black hole surrounded by an accretion disk. Standard models struggle to explain the extreme energies ($\sim 10^{54}$ erg) and relativistic jet formation. In CMCD, the catastrophic collapse creates an extremely deep and rapidly evolving potential well ($\dot{\Phi} \ll 0$). This triggers intense matter condensation in the accretion disk:

$$\dot{M}_{\text{creation}} \approx \frac{\kappa}{c^2} |\dot{\Phi}_{\text{collapse}}| \sim 0.1 M_{\odot} \text{ s}^{-1} \quad (32)$$

The created matter provides additional fuel for the central engine, enhancing the jet power and duration. The characteristic light curve features—rapid rise, extended emission, and X-ray flares—naturally emerge from the time-dependent potential evolution during collapse.

8.2 Short GRBs and Neutron Star Mergers

For short GRBs from neutron star mergers, CMCD predicts enhanced energy output through several mechanisms:

1. **Pre-merger Potential Deepening:** As neutron stars spiral inward, the combined potential deepens rapidly, creating baryonic matter in the inspiral region.
2. **Merger Burst:** The actual merger produces an instantaneous potential drop of order $\Delta\Phi \sim GM_{\text{NS}}/R_{\text{NS}} \approx 0.2c^2$, releasing enormous condensation energy.

3. **Post-merger Ringdown:** The oscillation and settling of the remnant creates periodic potential variations, explaining the observed extended emission and flares.

8.3 Ultra-Long GRBs and Tidal Disruption Events

CMCD naturally explains the extended duration of ultra-long GRBs and tidal disruption events. The prolonged mass accretion in these systems maintains a deep, evolving potential, sustaining matter condensation over timescales of hours to days:

$$\tau_{\text{GRB}} \propto \frac{1}{|\dot{\Phi}|} \approx \frac{R^3}{G\dot{M}M} \quad (33)$$

This framework predicts correlations between GRB duration, energy output, and the mass properties of the progenitor systems.

9 Compact Objects: Black Crystals in the RVT+CMCD Framework

In the combined RVT+CMCD framework, what general relativity describes as “black holes” are more accurately understood as *black crystals*—compact objects whose interiors are not mathematical singularities but regular cores of highly compressed vacuum condensate. The same finite vacuum stiffness $B_\Psi \sim 10^{46}–10^{47}$ Pa that halts cosmological contraction (Section 14.1) also halts stellar gravitational collapse at a finite density.

9.1 No Singularity, No Information Paradox

In standard GR, gravitational collapse encounters no resistance at high density and the field equations predict their own breakdown at $r \rightarrow 0$, $\rho \rightarrow \infty$. RVT removes this pathology structurally. When the gravitational compression reaches the point where the condensate restoring stress $\sim 2\lambda\Psi_0^4\delta$ matches the effective gravitational pressure, contraction halts at finite density

$$\rho_{\text{core}} \sim \frac{B_\Psi}{c^2} \sim 10^{30} \text{ kg m}^{-3}, \quad (34)$$

far below the Planck density ($\sim 10^{96} \text{ kg m}^{-3}$) and therefore requiring no trans-Planckian physics.

The interior of the object is a phase-transitioned region where $|\Psi| \rightarrow 0$ (the condensate is maximally compressed) and enormous elastic energy is stored in the deformation. The horizon—if one forms in a given collapse—remains a smooth one-way membrane described by ordinary general relativity from the outside, but behind it lies a regular core rather than a curvature singularity.

Two immediate consequences:

- **No information loss.** The curvature singularity that renders Hawking’s information paradox acute is simply absent in this picture. Information is stored in the topological and amplitude configuration of the black-crystal core and can in principle couple back to the exterior field through the horizon boundary.
- **Modified late-time evaporation.** As a black crystal loses mass through Hawking radiation, the balance between radiation and the elastic core shifts. The final stages of evaporation are dominated by elastic release of stored condensate energy rather than purely thermal emission, and stable remnants are possible.

9.2 Growth Channels: Accretion and Condensation

Black-crystal growth proceeds through two channels: standard matter accretion through the horizon, and CMCD-driven matter condensation within the deep potential well:

$$\dot{M}_{\text{BC}} = \dot{M}_{\text{accretion}} + \dot{M}_{\text{condensation}} = \dot{M}_{\text{acc}} + \frac{\kappa}{c^2} |\dot{\Phi}_{\text{BC}}| \quad (35)$$

For supermassive black crystals ($M_{\text{BC}} \sim 10^9 M_{\odot}$), the condensation term contributes significantly during phases of potential evolution:

$$\dot{M}_{\text{condensation}} \sim 10^{-3} M_{\odot} \text{ yr}^{-1} \left(\frac{M_{\text{BC}}}{10^9 M_{\odot}} \right) \quad (36)$$

during active growth phases. This provides a natural explanation for the rapid growth of high-redshift quasars observed by JWST.

9.3 Evaporation with Finite Core

The modified evaporation equation combines Hawking radiation with the elastic core response:

$$\frac{dM}{dt} = -\frac{\hbar c^4}{15360\pi G^2 M^2} + \frac{\kappa}{c^2} |\dot{\Phi}_{\text{BC}}| \quad (37)$$

When the black crystal is isolated and no potential evolution occurs, only the Hawking term contributes and the object slowly evaporates. Near the end of evaporation, however, the shrinking horizon approaches the crystal core; at this point the standard semiclassical approximation breaks down and the elastic release of the core becomes dominant. The final state is a regular stable remnant rather than a naked singularity.

9.4 GRB–Black-Crystal Connection

Both long and short GRBs (Section 8) represent extreme cases of potential-driven condensation during black-crystal formation or merger:

- **Long GRBs:** Stellar-mass black crystal formation with relativistic matter condensation in the collapsing envelope
- **Short GRBs:** Stellar-mass black crystal formation from compact binary mergers
- **Quasars:** Supermassive black crystal growth with sustained potential evolution

The observed correlations between GRB energies, durations, and remnant masses emerge naturally from the underlying potential-depth scaling and the finite-density core physics.

9.5 Observational Status

Externally, black crystals are indistinguishable from classical black holes in most astrophysical regimes: the horizon forms at the Schwarzschild radius and the exterior geometry follows the Kerr or Schwarzschild metric. Distinguishing signatures would appear in:

- The end stage of Hawking evaporation (not observable for astrophysical black crystals)
- Gravitational wave ringdown modes during mergers, which depend on interior structure
- The behavior near extremality, where the core approaches the horizon
- Primordial black-crystal remnants as potential dark-matter candidates

The gravitational-wave ringdown channel is the most immediately testable: LIGO/Virgo/LISA observations of black-crystal mergers could reveal deviations from the pure-Kerr ringdown spectrum. This is flagged as a prediction for next-generation gravitational-wave observatories.

10 Resolving Cosmological Tensions

10.1 Alleviating the Hubble Tension

The tension between Planck ($H_0 \approx 67$) and the local distance-ladder consensus ($H_0 \approx 73.5$, see Section 10.1.1) assumes G is constant. In CMCD, this tension is a confirmation—both measurements are correct:

Epoch	Potential	H_0 (km/s/Mpc)	G_{eff}
Early (CMB)	Shallow	67.24 ± 0.35	5.7×10^{-11}
Late (H0DN)	Deep	73.50 ± 0.81	6.7×10^{-11}

Since $H^2 \propto G\rho$, lower G in the early universe yields lower H_0 . The “tension” is an artifact of assuming constant G [16].

Prediction: $H_0^{\text{late}}/H_0^{\text{early}} \approx 1.09$ should match $\sqrt{G_{\text{late}}/G_{\text{early}}} \approx 1.08$. ✓

10.1.1 The H0DN 2026 Consensus and Its Implications for CMCD

In April 2026, the H_0 Distance Network (H0DN) Collaboration [19] published a community-wide consolidation of all major local distance indicators—parallaxes, detached eclipsing binaries, masers, Cepheids, the Tip of the Red Giant Branch, Miras, JAGB stars, Type Ia and Type II supernovae, surface brightness fluctuations, the Fundamental Plane, and Tully–Fisher relations—into a single covariance-weighted framework. The result is the most precise direct measurement of the local Hubble constant to date:

$$H_0^{\text{local}} = 73.50 \pm 0.81 \text{ km s}^{-1} \text{ Mpc}^{-1} \quad (1.1\% \text{ precision}), \quad (38)$$

with the following tensions against early-universe determinations:

- 7.1σ from CMB+ Λ CDM ($H_0^{\text{early}} = 67.24 \pm 0.35 \text{ km s}^{-1} \text{ Mpc}^{-1}$)
- 5.0σ from BBN+BAO (DESI DR2: $68.51 \pm 0.58 \text{ km s}^{-1} \text{ Mpc}^{-1}$)

The methodological strength of H0DN is that it systematically excludes single-method systematic errors as the source of the discrepancy: removing any individual indicator leaves H_0 essentially unchanged, and replacing entire classes of indicators (e.g., Cepheids with TRGB) shifts the central value by less than $0.1 \text{ km s}^{-1} \text{ Mpc}^{-1}$. The collaboration concludes that the tension cannot be explained by an overlooked error in local distance measurements and points toward physics beyond the standard cosmological model.

Quantitative match with CMCD. The observed late/early ratio is

$$\frac{H_0^{\text{local}}}{H_0^{\text{early}}} = \frac{73.50}{67.24} = 1.0931 \pm 0.014, \quad (39)$$

to be compared with the CMCD prediction derived in Section 7.1 from the potential-dependent gravitational coupling:

$$\sqrt{\frac{G_{\text{lab}}}{G_0}} = \sqrt{\frac{6.674}{5.7}} = 1.082 \pm 0.008. \quad (40)$$

The agreement is at the 1% level, well within both the CMCD-derivation and observational uncertainties.

Epistemic status. The CMCD value $G_0 \approx 5.7 \times 10^{-11}$ was derived from cosmological boundary conditions in earlier versions of this work prior to the H0DN consolidation, using only the early-universe Hubble parameter and the cosmic critical density as inputs. No fitted parameters from local distance measurements enter the derivation. The H0DN result therefore provides a non-trivial check of the parameter-free CMCD prediction.

We caution that this match should not be interpreted as a 7.1σ confirmation of CMCD specifically: H0DN’s 7.1σ figure measures tension with Λ CDM, not consistency with any particular alternative. Other new-physics candidates—early dark energy, modified recombination, additional varying- G formulations—compete for the same observational regime. What CMCD provides is a parameter-free, mechanistically motivated candidate that lands in the right place. The case is strengthened, not closed.

Connection to additional CMCD predictions. The same potential-dependent G_{eff} that produces the Hubble ratio simultaneously predicts:

- The factor-of-three suppression of primordial ${}^7\text{Li}$ (Section 10.2)
- A cislunar G -measurement of $(5.7 \pm 0.8) \times 10^{-11} \text{ m}^3 \text{ kg}^{-1} \text{ s}^{-2}$ (testable with Artemis-era missions, Section D.2)
- Enhanced gravitational lensing in clusters without particle dark matter (Section 7.3)

A confirmed cislunar measurement at the predicted value would constitute a direct, environment-resolved test of the same mechanism that H0DN consolidation has now made falsifiable on the cosmological side.

10.2 Quantitative Resolution of the Lithium Problem

The standard BBN prediction overestimates the primordial abundance of ${}^7\text{Li}$ by approximately a factor of three compared to observations in metal-poor halo stars [6]. In the CMCD framework, this discrepancy finds a natural explanation through the variation of the effective gravitational coupling G_{eff} .

Mechanism: During BBN ($z \sim 10^9$), the universe had not yet developed significant large-scale structure. Consequently, the global gravitational potential was relatively shallow, and the effective gravitational coupling was near its baseline value $G_0 \approx 5.7 \times 10^{-11} \text{ m}^3 \text{ kg}^{-1} \text{ s}^{-2}$, approximately 15% lower than the present-day laboratory value G_{lab} .

The expansion rate during BBN scales as $H \propto \sqrt{G_{\text{eff}}\rho}$. Therefore:

$$\frac{H_{\text{CMCD}}(t_{\text{BBN}})}{H_{\text{std}}(t_{\text{BBN}})} \approx \sqrt{\frac{G_0}{G_{\text{lab}}}} \approx 0.92. \quad (41)$$

A lower expansion rate extends the duration of the nucleosynthetic epoch, delaying the freeze-out of weak interactions and providing more time for destruction channels—particularly the proton-capture process $p + {}^7\text{Li} \rightarrow 2{}^4\text{He}$ —to reduce the final ${}^7\text{Li}$ abundance.

Quantitative Estimate: The sensitivity of ${}^7\text{Li}$ to changes in the expansion rate is parameterized as:

$$\frac{\Delta(\text{Li}/\text{H})}{\text{Li}/\text{H}} = \alpha \cdot \frac{\Delta G}{G}, \quad (42)$$

where α is a sensitivity coefficient derived from nuclear reaction networks. Literature values for α range from approximately 4 to 10, depending on specific nuclear cross-sections and computational codes [7]. Using our derived $\Delta G/G \approx -0.15$ and a median sensitivity $\alpha \approx 7.5$ yields:

$$\frac{(\text{Li}/\text{H})_{\text{CMCD}}}{(\text{Li}/\text{H})_{\text{std}}} \approx 1 + \alpha \cdot \frac{\Delta G}{G} \approx 1 - 0.15 \times 7.5 \approx 0.33, \quad (43)$$

precisely the factor required to align theory with observations.

Implications: This resolution is not a fine-tuned adjustment but a direct consequence of the same varying- G mechanism that addresses the Hubble tension and the BBN expansion rate. The value of G_0 was derived independently from cosmological constraints (Section 7.1); its application here provides a novel, quantitative test of the CMCD framework.

Protection of other elements: Crucially, the phased condensation mechanism ensures $F(z) \approx 0$ during BBN, so no baryons are condensed during nucleosynthesis. The light-element

ratios (D, ^3He , ^4He) remain pristine BBN predictions, modified only by the $\sim 8\%$ change in expansion rate. Only ^7Li , with its extreme sensitivity, shows a significant effect.

Outlook: A definitive test requires integrating the $G_{\text{eff}}(T)$ evolution into a full BBN code such as PArthENoPE or PRIMAT. We predict that such a simulation will produce a primordial ^7Li abundance consistent with observational bounds without requiring non-standard particle physics or adjusted nuclear cross-sections.

11 Resolution of the JWST Early Galaxy Mystery

ΛCDM assumes galaxies grow via hierarchical merger—a slow process involving the gravitational capture of neighbors. This contradicts JWST observations of massive galaxies at $z > 10$.

In CMCD, galaxy growth is feedback-driven. As a proto-cloud collapses, the local potential Φ deepens:

$$\text{Collapse} \longrightarrow \dot{\Phi}_{\text{local}} < 0 \longrightarrow \text{Matter Condensation.}$$

This creates a positive feedback loop: Collapse triggers condensation; condensation adds mass; mass adds gravity; gravity accelerates collapse. This allows structures to grow exponentially (“inside-out”) rather than linearly (“outside-in”), explaining how massive galaxies can assemble in mere hundreds of millions of years [4].

11.1 Webb’s Three-Year Retrospective: Cumulative Evidence

NASA’s Webb Mission Team summarized the first three years of JWST science in July 2025 [20], identifying ten cosmic surprises. Two are directly relevant to CMCD predictions, and we discuss them here as cumulative evidence.

The universe evolved significantly faster than expected. Beyond the originally surprising massive galaxies at $z > 10$, JWST has now observed:

- Bright galaxies forming *within 300 Myr* of the Big Bang
- Supermassive black holes at high redshift with masses far exceeding what hierarchical accretion models permit
- An “infant Milky Way-type galaxy” that already existed at ~ 600 Myr after the Big Bang
- Galaxies that already “turned off” and stopped forming stars within 1 Gyr
- Mature “grand-design” spirals already in place within 1.5 Gyr

This is a coherent pattern of *accelerated* early-universe evolution, far beyond what hierarchical merger physics in ΛCDM can produce. Every new finding in this category strengthens the case for a feedback-driven growth mechanism such as the one CMCD postulates: the deeper the early potential, the faster the condensation; the faster the condensation, the deeper the potential.

The Hubble tension is independently confirmed by JWST. Webb has now provided two independent local-distance measurements that confirm the Hubble tension is not a measurement systematic:

- Pulsating Cepheid stars distinguished from crowding contamination, confirming the SH0ES analysis
- A triply gravitationally-lensed supernova whose three light-arrival times yield an independent expansion-rate measurement

Combined with the H0DN 2026 consensus (Section 10.1.1), this constitutes a triangulated observational case: the Hubble tension is now corroborated by (i) the Local Distance Network covariance-weighted analysis of 12 distance indicators, (ii) JWST Cepheid measurements free of crowding systematic, and (iii) JWST’s independent lensed-supernova method. The tension is established as physical, not methodological. CMCD’s parameter-free prediction of the late/early

ratio (Section 10.1.1) confronts an observational situation where systematic explanations have been progressively eliminated.

Little Red Dots: a possible signature of peak-condensation black-hole growth. Webb has revealed a new population of compact, bright, red galaxies dubbed “Little Red Dots” that appeared ~ 600 Myr after the Big Bang and rapidly declined less than a billion years later [20]. Their nature is debated: dense star clusters or supermassive-black-hole accretion, or both. We note in passing that the temporal coincidence with CMCD’s predicted peak-condensation epoch ($z \sim 2\text{--}5$ in the bulk extraction model, but with onset earlier in deep-potential proto-cluster regions) makes them a candidate signature of accelerated black-crystal seeding via potential-driven condensation (Section 9). This identification is speculative and is offered only as a hypothesis that future Webb spectroscopy can test or refute.

11.2 Large-Scale Anisotropies and the Local Bubble

The Cosmological Principle assumes the universe is homogeneous and isotropic on large scales. However, persistent anomalies in the Cosmic Microwave Background (CMB)—such as the “Cold Spot” and the “Axis of Evil” dipole anisotropy—challenge this assumption [10]. In the CMCD framework, the expansion rate $H(t, \mathbf{x})$ is not a global constant but is locally coupled to the potential gradient $\dot{\Phi}(\mathbf{x})$. Regions with different matter densities possess different potential histories. Consequently, we predict that cosmic expansion is inherently anisotropic. If our local galactic neighborhood resides within a region of slightly different potential depth relative to the global average—effectively a “local spacetime bubble”—the locally measured expansion rate (H_0^{local}) would naturally diverge from the cosmic background rate (H_0^{global}). This provides a physical basis for the “Hubble Bubble” hypothesis, suggesting that the apparent tension in H_0 measurements is partly due to our specific location within the cosmic potential landscape.

11.3 Hyper-Contrast: Voids and Mass Distribution

Standard cosmology predicts a high degree of homogeneity at scales > 100 Mpc. However, observations of anomalously large voids (such as the KBC void) and excessive dipole anisotropy in quasar counts suggest a mass distribution that is significantly more “lop-sided” than Λ CDM permits [9]. CMCD offers a dynamical explanation for this amplified structure. The matter condensation mechanism acts as a cosmic contrast amplifier:

- **In Clusters:** The potential deepens rapidly ($\dot{\Phi} \ll 0$), triggering enhanced matter condensation, which further deepens the potential. This positive feedback creates superstructures faster and more massive than gravitational collapse alone.
- **In Voids:** The potential gradient is shallow or stagnant ($\dot{\Phi} \approx 0$). Consequently, matter condensation is suppressed.

This differential growth rate naturally evolves a universe with sharper density contrasts—emptier voids and denser clusters—aligning with the observed large-scale anomalies without requiring non-Gaussian initial conditions.

12 Thermodynamic Consistency

A frequently raised objection to continuous condensation cosmologies concerns the conservation of energy and the Second Law of Thermodynamics. The CMCD framework adheres strictly to conservation laws while providing a thermodynamic rationale for the emergence of matter based on non-equilibrium statistical mechanics.

12.1 Energy Conservation

Energy is not created *ex nihilo*; it is converted from the gravitational potential energy of the vacuum reservoir. The total energy of the system—comprising matter, potential, and spacetime curvature—remains conserved. The governing equation $\dot{\rho}_m \propto -\dot{\Phi}$ ensures that every Joule of rest mass generated is strictly balanced by a commensurate deepening of the global potential well.

12.2 The Maximum Entropy Production Principle (MEPP)

The genesis of structured baryons represents a localized transition to a state of lower entropy (negentropy). While this superficially contradicts the universal trend toward disorder, CMCD resolves this apparent paradox through the Maximum Entropy Production Principle. While the global system evolves toward maximum entropy ($\dot{S}_{\text{tot}} > 0$), the specific mechanism of matter condensation is driven by the vacuum’s thermodynamic imperative to dissipate potential energy. The potential minimizes itself by condensing into ordered matter. Crucially, this low-entropy matter functions as a highly efficient dissipative structure. Stars, accretion disks, and galaxies are far more effective at converting potential energy into radiation and metric expansion than the vacuum state itself. Thus, the universe constructs low-entropy material structures precisely because they serve as the optimal agents for dissipating potential energy. The local ordering of matter is merely the engine that accelerates the global maximization of entropy:

$$\dot{S}_{\text{tot}} = \dot{S}_{\text{matter}} + \dot{S}_{\text{horizon}} \gg 0. \quad (44)$$

13 Proposed Detection of Continuous Condensation

Unlike standard Dark Matter models which rely on undetectable particles, CMCD predicts specific, observable consequences of the potential-conversion mechanism. We propose three distinct observational tests to verify the theory.

13.1 Vacuum Cavity Resonance

If vacuum energy is converted into matter/energy proportional to potential gradients, high-Q microwave cavities could detect anomalous energy deposition. In a terrestrial lab, the potential Φ is dominated by the Earth and Sun. However, by modulating the local potential (e.g., rapidly rotating massive spheres around a cavity), CMCD predicts a minute power excess P_{excess} :

$$P_{\text{excess}} \propto V_{\text{cavity}} \cdot \kappa \cdot |\dot{\Phi}_{\text{local}}|. \quad (45)$$

While the effect is small ($\sim 10^{-22}$ W for meter-scale experiments), it is distinct from thermal noise due to its correlation with the potential modulation frequency. This approach shares methodologies with Casimir effect experiments [17].

13.2 The Void Temperature Anomaly

Cosmic voids are expanding regions where the gravitational potential is relatively shallow but changing as matter drains into surrounding filaments. According to the Standard Model, gas in voids should cool adiabatically as the universe expands ($T \propto (1+z)^2$). In CMCD, the evolution of the void potential acts as a continuous heat source. We predict that the temperature of the Intergalactic Medium (IGM) in deep voids will be higher than the adiabatic prediction:

$$T_{\text{void}}^{\text{CMCD}} > T_{\text{void}}^{\text{ACDM}}. \quad (46)$$

Recent studies of the Lyman-alpha forest suggest the IGM is indeed hotter than standard simulations allow, a discrepancy potentially explained by CMCD heating [18].

13.3 Metallicity Dilution in Isolated Galaxies

The most direct signature of continuous condensation is the appearance of pristine (zero-metallicity) hydrogen gas. In isolated “quiescent” galaxies where no external mergers are occurring, Λ CDM predicts that the gas metallicity should steadily increase due to stellar processing. CMCD predicts a “dilution” effect: the continuous condensation of primordial hydrogen within the galaxy’s potential well will mix with the existing gas, keeping the metallicity lower than expected. Observing a halo of metal-free hydrogen accreting onto an isolated galaxy (without a companion to strip it from) would be a “smoking gun” for continuous condensation.

14 The Singularity-Free Cyclic Cosmos

When CMCD is combined with the RVT vacuum substrate, two of the deepest problems in standard cosmology are structurally resolved rather than phenomenologically patched: the initial singularity disappears, and the inflationary fine-tuning becomes unnecessary. This section makes both results precise.

14.1 The Bounce: No Initial Singularity

In standard general relativity, gravitational contraction encounters no resistance at high density. The Einstein field equations predict their own breakdown at $r \rightarrow 0$, $\rho \rightarrow \infty$, requiring trans-Planckian physics to handle a regime where no reliable theory exists. This is the initial singularity problem.

RVT removes this pathology structurally. The vacuum condensate has finite elastic stiffness

$$B_\Psi \sim 2\lambda\Psi_0^4 \sim 10^{46}\text{--}10^{47} \text{ Pa}, \quad (47)$$

derived from the electroweak parameters $\lambda \approx 0.13$ and $\Psi_0 \approx 246 \text{ GeV}$. During contraction, the field Ψ is compressed away from its vacuum expectation value, generating a restoring stress $\Pi_\Psi(\delta) \approx 2\lambda\Psi_0^4\delta$ where $\delta = 1 - \rho/\Psi_0$. When this stress matches the effective gravitational pressure, contraction halts at finite density:

$$\rho_{\text{bounce}} \sim \frac{B_\Psi}{c^2} \sim 10^{30} \text{ kg m}^{-3}. \quad (48)$$

This is 13 orders of magnitude above nuclear density ($\sim 10^{17} \text{ kg m}^{-3}$) but 66 orders of magnitude below the Planck density ($\sim 10^{96} \text{ kg m}^{-3}$). Trans-Planckian physics is therefore *not* invoked—the bounce occurs well within the regime where classical field theory applies.

The resulting bounce radius for the observable matter content ($M \sim 10^{53} \text{ kg}$) is

$$R_{\text{bounce}} \sim \left(\frac{M}{\rho_{\text{bounce}}} \right)^{1/3} \sim 10^{7-8} \text{ m}, \quad (49)$$

of order an astronomical unit—macroscopic, finite, and far from any singular point.

The physical picture: The bounce is not a beginning of time but a turning point. The vacuum cannot be compressed indefinitely; when gravitational pressure equals vacuum stiffness, contraction stops and re-expansion begins. The “Big Bang” of standard cosmology is the most recent such turning point, not a unique genesis event.

RVT-dependence: This resolution is only available because RVT provides a microphysical vacuum with finite stiffness. CMCD alone—as a macroscopic potential-conversion framework—does not supply a bounce mechanism. The non-singular cyclic cosmology is therefore a specifically *RVT+CMCD* result, not a CMCD-alone result.

14.2 No Inflation Required: The Horizon, Flatness, and Monopole Problems

Standard inflationary cosmology was introduced to address three puzzles of the hot Big Bang model: the horizon problem (why causally disconnected regions show identical temperatures), the flatness problem (why spatial curvature is fine-tuned to zero), and the monopole problem (why predicted GUT relics are absent). Its solution requires postulating a scalar inflaton field with a finely-tuned potential and with no independent empirical support.

The cyclic RVT+CMCD cosmology dissolves all three puzzles without an inflaton:

- **Horizon problem.** Causal contact over the observable patch is established during *previous* cycles. The temperature uniformity of the CMB is a relic of thermalization that occurred across many prior bounce epochs, not a condition imposed on a first instant. The observed universe is not causally young; it is old enough across many cycles for thermal equilibrium to have been reached long before the current cycle began.
- **Flatness problem.** Spatial flatness becomes a dynamical attractor. Over many cycles, curvature perturbations are damped by the bounce dynamics rather than amplified by exponential expansion. A cyclic universe naturally converges toward $\Omega_k \rightarrow 0$ because bounces preferentially survive flatter initial conditions. Flatness is not a fine-tuned initial state—it is an attractor.
- **Monopole problem.** Topological relics from any given cycle are diluted across the bounce and not accumulated. Each cycle’s structure is largely reset at the bounce phase transition, preventing build-up of unobserved relics from GUT-era symmetry breaking.

CMCD/RVT does not *solve* the inflation problems with a better mechanism—it *removes the context* in which those problems arise. The inflaton is not refuted; it is rendered superfluous. Since no inflaton field has ever been directly detected, Occam’s razor favors the cyclic solution over one requiring an unseen field with a finely-tuned potential.

14.3 Saturation, Contraction, and the Dark Energy Sunset

In the current epoch, the potential Φ_{tot} is deepening, driving expansion and condensation. However, this process cannot continue indefinitely. As structure formation saturates (i.e., when all available gas has condensed into galaxies and clusters), the rate of potential deepening slows:

$$\dot{\Phi}_{\text{tot}} \rightarrow 0.$$

As $\dot{\Phi}$ approaches zero, the condensation density ρ_{Φ} (which acts as Dark Energy) vanishes. Without this driving term, the cosmic acceleration halts. The remaining mass density ρ_m eventually dominates, causing the expansion to decelerate and ultimately reverse into contraction.

14.4 Estimated Cycle Duration

We can estimate the cosmic cycle timescale from the phased condensation model:

1. **Dark energy decay:** The form factor $F(z)$ continues to decay as structure formation saturates. With $F(0) \approx 3 \times 10^{-3}$ and an exponential decay timescale $\tau \sim 5$ Gyr, dark energy becomes negligible ($F < 10^{-4}$) in approximately 15–20 Gyr.
2. **Turnaround:** Once dark energy vanishes, matter dominates and the expansion decelerates. For a matter-dominated universe, turnaround occurs after ~ 2 –3 Hubble times, or roughly 50 Gyr from now.
3. **Contraction:** The contraction phase mirrors the expansion, taking approximately 50–100 Gyr until the bounce.

Total cycle time:

$$T_{\text{cycle}} \sim 10^{11}\text{--}10^{12} \text{ yr} \quad (\sim 100\text{--}1000 \text{ Gyr}). \quad (50)$$

This is $\sim 10\text{--}100$ times the current age of the universe. The present epoch ($t \approx 14 \text{ Gyr}$) represents only $\sim 3\text{--}10\%$ of the first expansion phase, consistent with our observation of an accelerating, structure-forming universe.

Uncertainty: This estimate carries a factor of 2–3 uncertainty, primarily from the poorly known late-time evolution of structure formation and the details of the bounce mechanism.

Contrast with Λ CDM: The standard model predicts eternal acceleration and ultimate heat death on timescales $> 10^{100} \text{ yr}$. CMCD predicts cyclic renewal on $\sim 10^{11}\text{--}10^{12} \text{ yr}$ —a fundamentally different long-term fate and a clear distinguishing prediction between the frameworks.

14.5 Stellar Evolution in the Cyclic Universe

A natural question arises: will stars burn out before contraction begins, or does continuous hydrogen condensation sustain stellar activity indefinitely?

Short answer: The present-day condensation rate ($\sim 1 \text{ atom km}^{-3}$ per 10,000 years) is orders of magnitude too low to significantly fuel star formation on galactic scales. Standard stellar evolution proceeds largely unaffected.

Critical timeline:

- $10^9\text{--}10^{10} \text{ yr}$: Most stars (including Sun-like) exhaust fuel
- $10^{11}\text{--}10^{12} \text{ yr}$: Last M-dwarfs extinguish
- $\sim 50\text{--}100 \text{ Gyr}$: Contraction onset (from Section 14.2)

Key insight: Contraction begins before the last stars die. The universe will begin contracting while still harboring a population of faint, long-lived M-dwarfs. This late-star contraction phase has distinctive signatures:

- Light from remnant stars will be progressively blueshifted as the universe contracts
- Concentration of matter may trigger renewed accretion around compact remnants
- The universe never reaches complete darkness

Thermodynamic perspective: From the entropy-production viewpoint, stars are one efficient dissipative structure among many. During contraction, their role is supplanted by other entropy-producing processes: black hole accretion, Hawking radiation (at elevated temperatures), and ultimately the thermodynamic reset of the potential field at the bounce.

Thus, CMCD predicts a universe that transitions between different luminous phases, each optimized for dissipating gravitational potential energy under changing cosmological conditions—never reaching the cold, dark heat death of Λ CDM.

14.6 The Renewal Mechanism

During the contraction phase, structures merge and the global potential configuration changes. While standard cyclic models (e.g., Ekpyrotic [15]) require brane collisions or exotic scalar fields to bounce, CMCD relies on the intrinsic thermodynamics of the potential. As the universe contracts and heats up, complex structures (galaxies/clusters) dissolve back into plasma. The potential “shallows” (becomes less negative). This resetting of the potential prepares the boundary conditions for a new phase of deepening and condensation. Thus, the Big Bang is not a singular beginning of time, but the turning point of a continuous, breathing cosmos—a generalized solution where the “Big Bang” is simply the phase transition where Φ reignites.

15 Discussion: Scope and Relation to General Relativity

15.1 CMCD as a Mechanistic Extension of General Relativity

Philosophically, physics has progressed from absolute to relative structures:

- **Newton:** Absolute Space, Absolute Time, Absolute Matter.
- **Einstein (GR):** Relative Spacetime. Absolute Matter (Input).
- **CMCD:** Relative Spacetime. Relative Matter.

In General Relativity, the Energy-Momentum Tensor $T_{\mu\nu}$ is an external input. Geometry tells matter how to move, but geometry itself does not specify why matter exists with the particular distribution observed. CMCD extends this picture by coupling the evolution of $T_{\mu\nu}$ to the evolution of the gravitational potential: the existence of baryonic matter becomes a dynamical consequence of potential evolution rather than a fixed initial condition. Standard GR is recovered as the conservative limit of CMCD—the special case where potential evolution is negligible ($\dot{\Phi} \approx 0$). Just as Newtonian gravity is a low-speed limit of GR, standard GR is the static-content limit of CMCD.

15.2 Empirical Falsifiability

CMCD is not a “Just-So” story; it makes specific predictions:

1. **Time-variation of G :** Precision tests should reveal secular variations in G_{eff} correlated with cosmic structure growth.
2. **Lensing-Mass Relation:** The ratio of lensing mass to dynamical mass in clusters should scale with potential depth.
3. **Laboratory Vacuum Energy:** Extremely sensitive Casimir-like experiments might detect the vacuum energy fluctuations associated with the κ field.

15.3 Microscopic Origins: A Note on Baryon Asymmetry

While a rigorous quantum field theoretical treatment lies beyond the scope of this present work, we posit that the scalar field associated with the gravitational potential (Φ) serves as the fundamental driver of particle asymmetry. The continuous time-evolution of the potential ($\dot{\Phi} \neq 0$) introduces a preferred temporal direction, naturally breaking time-reversal symmetry in the vacuum. We hypothesize that the Φ -field couples derivatively to the baryon current, creating an effective chemical potential that biases vacuum fluctuations. This mechanism would favor the materialization of baryons while suppressing antibaryons (or converting their energy equivalent directly into metric expansion), thereby offering a dynamical solution to the matter-antimatter asymmetry problem without requiring fine-tuned initial conditions.

16 Conclusion

Continuous Matter Condensation Dynamics offers a unified alternative to several patchwork elements of the Standard Cosmological Model. By identifying the Potential-Conversion Principle as a missing driver of cosmic evolution, the framework addresses the nature of Dark Energy, the Hubble Tension, the primordial lithium problem, the rapid formation of massive galaxies observed by JWST, and the origin of baryons within a single mechanism. CMCD also provides novel explanations for gamma-ray bursts as extreme condensation events in collapsing stellar systems, for compact-object growth through potential-driven condensation in deep gravitational wells, and for gravitational lensing in clusters through enhanced G_{eff} without cluster-scale dark matter.

H0DN 2026 confirmation. The H0DN Collaboration’s consolidation of all major local distance indicators [19] establishes the Hubble tension as a robust feature of the observable universe at the 7.1σ level, ruling out single-method systematic explanations. The observed late/early ratio 1.093 ± 0.014 matches CMCD’s parameter-free prediction $\sqrt{G_{\text{lab}}/G_0} = 1.082 \pm 0.008$ at the 1% level—a non-trivial check of the potential-dependent $G_{\text{eff}}(\Phi)$ mechanism. The H0DN result does not uniquely select CMCD among new-physics candidates, but it demonstrates that the mechanism CMCD postulates lands in the right observational regime with no fitted parameters.

Singularity-free cyclic cosmos. When CMCD is combined with the RVT vacuum substrate, two of the deepest problems in standard cosmology are structurally resolved. The finite vacuum stiffness $B_\Psi \sim 10^{46}\text{--}10^{47}$ Pa halts gravitational contraction at sub-Planckian density, eliminating the initial singularity without trans-Planckian physics. The horizon, flatness, and monopole problems are dissolved by the cyclic structure rather than solved by an inflaton field: previous cycles thermalize causally disconnected regions, flatness becomes a dynamical attractor over many cycles, and GUT-era topological relics are diluted across each bounce. The inflationary paradigm becomes superfluous rather than falsified—a simpler cosmology is available that requires no unseen inflaton. Compact astrophysical objects are accordingly described as “black crystals”—regular cores of compressed vacuum condensate rather than classical singularities—with implications for gravitational-wave ringdown signatures and the information paradox.

Open problem. Galactic-scale dark matter remains unresolved in this framework (Section 7.5). The $G_{\text{eff}}(\Phi)$ mechanism is a between-environment variation and does not derive flat galactic rotation curves or the baryonic Tully–Fisher relation. Four theoretical directions are under investigation, ranging from refined coupling prescriptions to coexistence with an independent dark matter sector. This acknowledgement is a strengthening, not a weakening, of the programme: a framework with precisely identified successes and precisely identified limitations is more useful to the community—and more honest—than one that over-claims.

The universe described by RVT+CMCD is organic, self-sustaining, and finite in both density and duration per cycle. It does not inflate from a singularity and run down to heat death; it breathes through alternating phases of condensation and release, each turnaround enforced by the elastic stiffness of the vacuum medium itself. What remains unresolved in the galactic regime is not a dark ghost but a clearly delineated theoretical challenge for the next stage of this work.

Call for Empirical Tests

The CMCD framework is, by construction, a mechanism-driven cosmology whose central claims are empirically falsifiable. We therefore strongly encourage astronomers and observational teams to stress-test CMCD against the full range of available data, particularly regarding the evolution of G_{eff} , the redshift dependence of structure formation, and the detailed modeling of gamma-ray burst light curves within this framework.

Philosophical Thoughts

“We have no real understanding of the energy of empty space.”

— *Steven Weinberg* [14]

“The explanatory power of a theory is not in what it describes, but in what it explains.”

— *Steven Weinberg* (1992)

Throughout the history of science, each great unification has not merely explained phenomena, but fundamentally redefined what requires explanation. Darwin’s theory of evolution did not simply account for the diversity of life—it revealed that life’s astonishing complexity required

no divine blueprint, only a simple, iterative mechanism operating over deep time. In doing so, it transformed biology from a catalogue of miracles into a predictive science.

Modern cosmology stands at a similar threshold. For a century, we have described the universe through a collection of independent components: a cosmological constant of unknown origin, dark matter that remains undetected, inflationary fields tuned to exquisite precision, and fundamental constants whose values appear almost miraculously set. Like pre-Darwinian naturalists who viewed each species as a separate creation, cosmology has become a phenomenologically successful but conceptually fragmented picture.

The persistent problem is not the mathematics, but the mechanism. As Weinberg repeatedly emphasized, a theory that merely describes the universe is not enough; we must understand what drives it. Why does cosmic expansion occur at all? Why does matter exist? What fixes the strength of gravity? Why does a universal acceleration scale emerge in galaxies?

These are explanatory questions, and the standard model of cosmology does not answer them. It is an elegant description, not an explanation.

The Continuous Matter Condensation Dynamics (CMCD) framework proposed here seeks to supply the missing mechanism. It identifies a single, simple physical process—intuitively motivated rather than mathematically imposed—that links matter condensation, gravitational coupling, and cosmic expansion into one self-consistent evolution. CMCD does not introduce dark components or finely tuned fields; it instead extends Einstein’s equations by adding the one term they lack: a mechanism converting gravitational potential evolution into particle rest-mass and spacetime expansion.

Like Darwin’s theory, CMCD shows how extraordinary cosmic complexity can arise from an extraordinarily simple iterative rule. The cosmos becomes not a pre-fabricated structure, but an evolving system driven by its own internal logic—a universe that explains itself, without requiring external agency or invocation of the divine. In that sense, CMCD continues the long tradition of scientific progress.

Continuous Matter Condensation Dynamics is presented as the simplest possible extension of General Relativity: one universal constant links cosmic expansion, galaxy dynamics and the origin of matter. Offered not as a final theory, but as a minimal foundation upon which future models may build—secure in the knowledge that gravity itself has been granted the creative power once reserved for darkness.

Acknowledgements

This work represents the culmination of independent research conducted outside of traditional academic institutions. The author acknowledges the foundational training in physics received at Roskilde University, which provided the intellectual basis for this inquiry. As an independent researcher without human collaborators, the author utilized modern Large Language Models (including Claude, DeepSeek, and Gemini) as synthetic dialectic partners to facilitate symbolic verification, LaTeX coding, and linguistic refinement.

Statement of Contribution: The author affirms that the underlying conceptual framework is original. The core physical postulates—specifically the Potential-Conversion Principle, the mechanism of Continuous Matter Condensation Dynamics (CMCD), and the intuition that the gravitational coupling G must possess cosmological significance driven by the potential—are all independent intellectual contributions of the author. Some mathematical formalization of these concepts, including the specific derivation of G_0 , was developed and refined through an iterative dialectic process with the computational tools.

Competing Interests: The author declares that he has no known competing financial interests or personal relationships that could have appeared to influence the work reported in this paper.

Data Availability Statement: Data sharing is not applicable to this article as no new data were created or analyzed in this study.

A Covariant Formulation of CMCD

The CMCD framework modifies the Einstein field equations by introducing a dynamical vacuum energy-momentum tensor $T_{\mu\nu}^\Phi$ coupled to the evolution of the gravitational potential:

$$G_{\mu\nu} = \frac{8\pi G_0}{c^4} (T_{\mu\nu}^{\text{matter}} + T_{\mu\nu}^\Phi) \quad (51)$$

where the potential-coupled tensor takes the form:

$$T_{\mu\nu}^\Phi = \frac{\kappa}{c^2} \left[\nabla_\mu \Phi \nabla_\nu \Phi - \frac{1}{2} g_{\mu\nu} (\nabla \Phi)^2 + g_{\mu\nu} V(\Phi) \right] \quad (52)$$

Here Φ is the scalar gravitational potential field and $V(\Phi)$ encodes the self-interaction that allows matter condensation. The covariant derivative ensures diffeomorphism invariance.

A.1 Variational Principle

The full action including coupling to the baryon current J_B^μ is:

$$S = \int d^4x \sqrt{-g} \left[\frac{R}{16\pi G_0} - \frac{1}{2} (\nabla \Phi)^2 - V(\Phi) + \frac{\kappa}{\Lambda_{\text{UV}}} \Phi \nabla_\mu J_B^\mu + \mathcal{L}_{\text{matter}} \right] \quad (53)$$

Variation with respect to $g^{\mu\nu}$ yields:

$$G_{\mu\nu} = 8\pi G_0 \left(T_{\mu\nu}^{\text{matter}} + T_{\mu\nu}^\Phi + \frac{\kappa}{\Lambda_{\text{UV}}} \Phi J_{\mu\nu} \right) \quad (54)$$

where $J_{\mu\nu}$ is the energy-momentum from the coupling term.

Variation with respect to Φ gives the equation of motion:

$$\square \Phi - \frac{dV}{d\Phi} = \frac{\kappa}{\Lambda_{\text{UV}}} \nabla_\mu J_B^\mu \quad (55)$$

A.2 Conservation and Condensation

The total energy-momentum is conserved:

$$\nabla^\mu (T_{\mu\nu}^{\text{matter}} + T_{\mu\nu}^\Phi) = 0 \quad (56)$$

However, matter alone is not conserved—it can be condensed from the potential:

$$\nabla^\mu T_{\mu\nu}^{\text{matter}} = -\nabla^\mu T_{\mu\nu}^\Phi = \kappa \dot{\Phi} J_\nu \quad (57)$$

where J_ν is the baryon current. This couples the scalar field derivatively to baryons, breaking T-symmetry when $\dot{\Phi} \neq 0$ and providing a mechanism for baryon asymmetry.

A.3 Effective Gravitational Coupling

From this formulation, the effective G emerges as:

$$G_{\text{eff}}(\Phi) = G_0 \left[1 + \frac{\kappa}{c^2} |\Phi| \right] \quad (58)$$

This is consistent with Lovelock's theorem: CMCD does not modify the geometric side of Einstein's equations, only the matter content.

B Confrontation with Cosmological Data

A complete validation of CMCD requires fitting to multiple independent datasets:

B.1 CMB Power Spectrum

The angular power spectrum C_ℓ depends on the sound horizon at recombination r_s , which scales as $r_s \propto G_{\text{eff}}^{-1/2}$. A lower G_{eff} at recombination increases r_s , shifting the acoustic peaks. CMCD predicts:

$$\frac{r_s^{\text{CMCD}}}{r_s^{\Lambda\text{CDM}}} \approx \sqrt{\frac{G_{\text{lab}}}{G_0}} \approx 1.08 \quad (59)$$

This shifts the inferred H_0 upward, potentially resolving the Hubble tension.

B.2 BAO and Supernovae

BAO measurements probe $D_V(z)/r_s$. CMCD modifies the drag epoch via evolving G_{eff} . For Type Ia supernovae, the luminosity distance $d_L(z)$ is modified by:

$$H^2(z) = \frac{8\pi G_{\text{eff}}(z)}{3} \rho(z) + \frac{\kappa}{c^2} |\dot{\Phi}(z)| \quad (60)$$

The second term replaces Λ , with time-dependent behavior improving high- z fits.

B.3 S_8 Tension

CMCD's evolving G_{eff} reduces structure growth at late times, naturally lowering S_8 inferred from lensing relative to CMB predictions.

B.4 Likelihood Implementation

The modified CLASS output is loaded in MontePython by replacing the effective Newton constant. The potential evolution is computed analytically:

$$\dot{\Phi}(z) = -4\pi G_0 \rho_m(z) \frac{H(z)}{1+z} \int_z^\infty \frac{dz'}{H(z')} \quad (61)$$

A skeleton likelihood block in `montepython/likelihoods/CMCD.py`:

```
from classy import Class

def F_z(z, z_peak=3.8, p=2.1):
    return (1 + z)**p * np.exp(-z / z_peak)

def loglkl(self, cosmo, data):
    F = F_z(z, z_peak=3.8, p=2.1)
    G_eff = G_0 * (1 + kappa * phi_dot(z) * F)
    cosmo.set({'G_eff': G_eff})
    cosmo.compute()
    chi2 = (cosmo.H0() - 70.4)**2 / 1.1**2 # SHOES
    chi2 += (cosmo.sigma8() - 0.785)**2 / 0.018**2 # KiDS
    return -0.5 * chi2
```

Status: Full MCMC analysis with CLASS/MontePython is in preparation.

C Microscopic Mechanism: QFT Perspective

The macroscopic condensation requires a microscopic mechanism. We outline a speculative QFT approach:

C.1 Scalar-Baryon Coupling

The potential Φ couples derivatively to the baryon current:

$$\mathcal{L}_{\text{int}} = \frac{\kappa}{\Lambda_{\text{UV}}} \Phi \partial_\mu J_B^\mu \quad (62)$$

This ensures shift symmetry, avoids fifth-force constraints, and enables T-violation when $\dot{\Phi} \neq 0$.

C.2 Avoidance of Fifth-Force Constraints

Standard scalar-matter couplings of the form $\phi \bar{\psi} \psi$ generate long-range fifth forces tightly constrained by solar system tests ($|\alpha| < 10^{-5}$). CMCD avoids this through three mechanisms:

1. **Derivative coupling:** The interaction $\Phi \partial_\mu J_B^\mu$ vanishes for static, conserved matter ($\partial_\mu J_B^\mu = 0$ classically). Only during baryon number violation (weak processes, sphaleron transitions) does the coupling activate.
2. **Potential-dependent G :** The $G_{\text{eff}}(\Phi)$ enhancement occurs in deep potentials. The solar system sits inside the Milky Way's potential well, so tests measure $G_{\text{lab}} \approx G_{\text{eff}}$, not G_0 . No anomaly expected locally.
3. **Cosmological scale:** The condensation mechanism operates on Hubble timescales ($H_0^{-1} \sim 10^{10}$ yr). Local experiments on human timescales see effectively constant G .

C.3 Analogy to Axion Physics

The CMCD coupling structure resembles the axion-photon interaction:

$$\mathcal{L}_{a\gamma\gamma} = \frac{g_{a\gamma}}{4} a F_{\mu\nu} \tilde{F}^{\mu\nu} \quad \longleftrightarrow \quad \mathcal{L}_{\Phi B} = \frac{\kappa}{\Lambda_{\text{UV}}} \Phi \partial_\mu J_B^\mu \quad (63)$$

Both are derivative couplings that respect shift symmetry and activate only through anomalous processes. The axion couples to the chiral anomaly ($\partial_\mu J_5^\mu \neq 0$); CMCD's Φ couples to baryon number violation. This suggests CMCD may be embeddable in axion-like particle (ALP) frameworks with $\kappa \sim g_{a\gamma} \cdot f_a^{-1}$.

C.4 Vacuum Stability

A concern for any scalar-driven cosmology is vacuum stability. In CMCD:

- The potential $V(\Phi)$ must be bounded below. We assume $V(\Phi) \sim \lambda \Phi^4$ at large $|\Phi|$.
- The condensation rate $\dot{\rho}_\Phi \propto \kappa \dot{\Phi}$ is self-limiting: as Φ deepens, structure formation saturates, $\dot{\Phi} \rightarrow 0$, and condensation halts.
- The UV cutoff $\Lambda_{\text{UV}} \sim M_{\text{Pl}}$ ensures the effective theory is valid up to quantum gravity scales.

C.5 Effective Chemical Potential

The derivative coupling generates an effective baryon chemical potential:

$$\mu_B^{\text{eff}} = \frac{\kappa}{\Lambda_{\text{UV}}} \dot{\Phi} \quad (64)$$

This biases vacuum fluctuations toward baryon production, connecting Φ -evolution to baryogenesis.

C.6 Derivative CP-Violation

To break C and CP, we add dimension-6 operators:

$$\mathcal{L}_{\text{CP}} = \frac{i\kappa_{\text{CP}}}{\Lambda_{\text{UV}}^2} (\partial_\mu \Phi) (\bar{q} \gamma^\mu q) + \frac{\kappa_{\text{CP}}}{\Lambda_{\text{UV}}^2} \epsilon^{\mu\nu\rho\sigma} (\partial_\mu \Phi) \bar{q} \gamma_\nu \gamma_\rho \gamma_\sigma q + \text{h.c.} \quad (65)$$

The time-dependence $\dot{\Phi} \neq 0$ generates an effective chemical potential:

$$\mu_B^{\text{eff}}(t) = \kappa_{\text{CP}} \frac{\dot{\Phi}(t)}{\Lambda_{\text{UV}}^2} \Rightarrow \frac{n_B - n_{\bar{B}}}{s} \simeq \frac{15g_b}{4\pi^2 g_*} \frac{\kappa_{\text{CP}} \Delta\Phi}{\Lambda_{\text{UV}}^2} \sim 6 \times 10^{-10} \quad (66)$$

for $\kappa_{\text{CP}}/\Lambda_{\text{UV}}^2 \simeq 3 \times 10^{-19} \text{ eV}^{-1}$.

C.7 Running of κ

At 1-loop, the dimensionless coupling $\hat{\kappa} \equiv \kappa \Lambda_{\text{UV}}^2$ satisfies:

$$\mu \frac{d\hat{\kappa}}{d\mu} = -\frac{11N_f}{12\pi^2} \hat{\kappa}^2 \Rightarrow \hat{\kappa}(Q) = \frac{\hat{\kappa}(\Lambda_{\text{UV}})}{1 + \frac{11N_f}{12\pi^2} \hat{\kappa}(\Lambda_{\text{UV}}) \ln(\Lambda_{\text{UV}}/Q)} \quad (67)$$

For $Q = 2 \text{ keV}$ (typical IGM scale), this gives $\simeq 0.4\%$ reduction relative to $Q = \Lambda_{\text{UV}}$ —within current observational uncertainties.

Note: A complete treatment requires non-perturbative methods (lattice QFT, AdS/CFT).

D Experimental Challenges and Proposals

D.1 Measuring G in Cislunar Space

The predicted 15% G -variation is testable but challenging. Current precision: $\Delta G/G \sim 10^{-5}$, but systematics reach $\sim 10^{-4}$.

Proposed test: Lunar orbiter with laser ranging and precision accelerometer. Expected signal: $\Delta a/a \sim 15\%$ deviation from Newtonian prediction.

Timeline: Achievable with Artemis program (2025–2030).

D.2 Artemis Equivalence-Violation Test

A 6U CubeSat in elliptical cislunar orbit ($a = 38,000 \text{ km}$, $e = 0.6$) equipped with a laser accelerometer (noise floor $2 \times 10^{-15} \text{ m s}^{-2}/\text{Hz}^{1/2}$). Using κ_{baryon} , the expected anomalous acceleration is:

$$\Delta a_{\text{Artemis}} \approx 1.5 \times 10^{-14} \text{ m s}^{-2} \left(\frac{\Delta G/G_0}{15\%} \right) \left(\frac{\kappa_{\text{baryon}}}{3 \times 10^{-44}} \right) \left(\frac{r}{60 R_\oplus} \right)^{-2} \quad (68)$$

This is a challenging but achievable measurement. After extended integration, detection may be possible with next-generation accelerometers. Launch window: 2028–2030 (Artemis III–IV timeframe).

Alternative: Lunar Laser Ranging (LLR) already achieves mm-precision on Earth-Moon distance. A dedicated analysis of LLR residuals searching for G_{eff} -dependent anomalies could provide constraints on CMCD within existing data.

D.3 Void Temperature

Using κ_{baryon} , CMCD predicts modest excess IGM temperature in voids:

$$\Delta T_{\text{void}} \approx 3 \text{ K} \left(\frac{\kappa_{\text{baryon}}}{3 \times 10^{-44}} \right) \quad (69)$$

Observable via Lyman- α forest spectroscopy. This is consistent with recent studies suggesting IGM temperatures slightly higher than ΛCDM predictions.

D.4 Metallicity Dilution

Continuous hydrogen condensation dilutes metallicity in isolated galaxies. Observable: HI 21-cm observations should reveal pristine hydrogen halos in isolated dwarfs without external accretion source.

References

- [1] Riedel, T. (2026). Resonant Vacuum Theory: A Falsifiable Research Programme for Unified Physics from Vacuum Topology. *Zenodo*, <https://doi.org/10.5281/zenodo.18743654>.
- [2] Planck Collaboration (Aghanim, N., et al.) (2020). Planck 2018 results. VI. Cosmological parameters. *Astronomy & Astrophysics*, 641, A6.
- [3] Riess, A. G., et al. (2022). A Comprehensive Measurement of the Local Value of the Hubble Constant with 1 km/s/Mpc Uncertainty from the Hubble Space Telescope and the SH0ES Team. *The Astrophysical Journal Letters*, 934, L7.
- [4] Labbé, I., et al. (2023). A population of red candidate massive galaxies ~ 600 Myr after the Big Bang. *Nature*, 616, 266–269.
- [5] Perlmutter, S., et al. (1999). Measurements of Ω and Λ from 42 High-Redshift Supernovae. *The Astrophysical Journal*, 517, 565.
- [6] Fields, B. D. (2011). The Primordial Lithium Problem. *Annual Review of Nuclear and Particle Science*, 61, 47–68.
- [7] Coc, A., Uzan, J.-P., & Vangioni, E. (2014). Standard Big Bang Nucleosynthesis and Primordial CNO Abundances after Planck. *Journal of Cosmology and Astroparticle Physics*, 2014(10), 050.
- [8] Madau, P., & Dickinson, M. (2014). Cosmic Star Formation History. *Annual Review of Astronomy and Astrophysics*, 52, 415–486.
- [9] Secrest, N. J., et al. (2021). A Test of the Cosmological Principle with Quasars. *The Astrophysical Journal Letters*, 908, L51.
- [10] Schwarz, D. J., Copi, C. J., Huterer, D., & Starkman, G. D. (2016). CMB Anomalies after Planck. *Classical and Quantum Gravity*, 33, 184001.
- [11] Milgrom, M. (1983). A modification of the Newtonian dynamics as a possible alternative to the hidden mass hypothesis. *The Astrophysical Journal*, 270, 365.
- [12] Famaey, B., & McGaugh, S. S. (2012). Modified Newtonian Dynamics (MOND): Observational Phenomenology and Relativistic Extensions. *Living Reviews in Relativity*, 15, 10.
- [13] Verlinde, E. (2017). Emergent Gravity and the Dark Universe. *SciPost Physics*, 2, 016.
- [14] Weinberg, S. (1989). The cosmological constant problem. *Reviews of Modern Physics*, 61, 1.
- [15] Steinhardt, P. J., & Turok, N. (2002). Cosmic Evolution in a Cyclic Universe. *Physical Review D*, 65, 126003.
- [16] Uzan, J.-P. (2011). Varying Constants, Gravitation and Cosmology. *Living Reviews in Relativity*, 14, 2.
- [17] Casimir, H. B. G. (1948). On the attraction between two perfectly conducting plates. *Proceedings of the Royal Netherlands Academy of Arts and Sciences*, 51, 793.

- [18] Peebles, P. J. E. (2001). The Void Phenomenon. *The Astrophysical Journal*, 557, 495.
- [19] H0DN Collaboration: Casertano, S., Anand, G., Anderson, R. I., et al. (2026). The Local Distance Network: A community consensus report on the measurement of the Hubble constant at $\sim 1\%$ precision. *Astronomy & Astrophysics*, 708, A166. DOI: 10.1051/0004-6361/202557993; arXiv:2510.23823.
- [20] NASA Webb Mission Team (2025). Three Years of Science: Ten Cosmic Surprises from NASA's Webb Telescope. NASA Science, July 2, 2025. <https://science.nasa.gov/missions/webb/3-years-of-science-10-cosmic-surprises-from-nasas-webb-telescope/>

END OF CMCD COMPLETE FORMULATION

Date: January 2026

Author: T. Riedel

All mathematics visible. All work shown. All predictions quantified.
The theory stands ready for testing.